LETTERS

The impact and recovery of asteroid 2008 TC_3

P. Jenniskens[1], M. H. Shaddad[2], D. Numan[2], S. Elsir[3], A. M. Kudoda[2], M. E. Zolensky[4], L. Le[4,5], G. A. Robinson[4,5], J. M. Friedrich[6,7], D. Rumble[8], A. Steele[8], S. R. Chesley[9], A. Fitzsimmons[10], S. Duddy[10], H. H. Hsieh[10], G. Ramsay[11], P. G. Brown[12], W. N. Edwards[12], E. Tagliaferri[13], M. B. Boslough[14], R. E. Spalding[14], R. Dantowitz[15], M. Kozubal[15], P. Pravec[16], J. Borovicka[16], Z. Charvat[17], J. Vaubaillon[18], J. Kuiper[19], J. Albers[1], J. L. Bishop[1], R. L. Mancinelli[1], S. A. Sandford[20], S. N. Milam[20], M. Nuevo[20] & S. P. Worden[20]

In the absence of a firm link between individual meteorites and their asteroidal parent bodies, asteroids are typically characterized only by their light reflection properties, and grouped accordingly into classes[1–3]. On 6 October 2008, a small asteroid was discovered with a flat reflectance spectrum in the 554–995 nm wavelength range, and designated 2008 TC_3 (refs 4–6). It subsequently hit the Earth. Because it exploded at 37 km altitude, no macroscopic fragments were expected to survive. Here we report that a dedicated search along the approach trajectory recovered 47 meteorites, fragments of a single body named Almahata Sitta, with a total mass of 3.95 kg. Analysis of one of these meteorites shows it to be an achondrite, a polymict ureilite, anomalous in its class: ultra-fine-grained and porous, with large carbonaceous grains. The combined asteroid and meteorite reflectance spectra identify the asteroid as F class[3], now firmly linked to dark carbon-rich anomalous ureilites, a material so fragile it was not previously represented in meteorite collections.

The asteroid was discovered by the automated Catalina Sky Survey telescope at Mount Lemmon, Arizona on October 6 06:39 UTC (ref. 4). Early orbital solutions showed an impact 19 h after discovery with a predicted impact location in the Nubian Desert of northern Sudan[5,6] (Table 1). Numerous astronomical observatories imaged the object until it entered the Earth's umbra on October 7 01:49 UTC. In the previous two hours, its brightness oscillated with an amplitude of 1.02 mag at main periods of 49.0338 ± 0.0007 s and 96.987 ± 0.003 s, and their harmonics, revealing that the asteroid was in a non-principal-axis rotation state[7]. The oscillation was centred on absolute visible magnitude $H = 30.9 \pm 0.1$ (using a phase angle slope parameter $G = 0.15$). This is a measure of the asteroid's size.

Table 1 | Orbital parameters of 2008 TC_3 used to calculate the approach path

Symbol	Parameter	Value
a	Semimajor axis	1.308201 ± 0.000009 AU
q	Perihelion distance	0.899957 ± 0.000002 AU
ω	Argument of perihelion	234.44897 ± 0.00008°
Ω	Longitude of ascending node	194.101138 ± 0.000002°
i	Inclination	2.54220 ± 0.00004°
T_p	Perihelion time	2008 November 20.3989 ± 0.0001 UT

These parameters are JPL solution 15; equinox J2000, 2008 October 07.0 TDB or Barycentric Dynamical Time. The astrometric position of 295 observations were used. This ephemeris, when projected to an altitude of 50 km, predicts an entry velocity of 12.42 km s^{-1} at a shallow 20° angle relative to the surface, with a perpendicular uncertainty in position of only ±100 m.

Eyewitnesses in Wadi Halfa and at Station 6 (a train station between Wadi Halfa and Al Khurtum, Sudan) in the Nubian Desert described a rocket-like fireball with an abrupt ending. Sensors aboard US government satellites first detected the bolide at 65 km altitude at 02:45:40 UTC (ref. 8). The optical signal consisted of three peaks spanning 3.5 s, with most of the radiated energy in the middle 1-s pulse at an inferred altitude of about 37 km, and a final pulse 1 s later. Meteosat 8 (ref. 9) detected the brightest optical signal when the asteroid was at 37.5 ± 1.0 km. Rapidly fading infrared radiation was detectable down until at least 32.7 ± 0.7 km. The 10-μm Si–O band of glowing dust was the dominant feature in a seven-channel 6–13 μm infrared spectrum taken ~1 s after the explosion. The height of the dust cloud was 35.7 ± 0.7 km. Independently, we measured this altitude at 35–42 km, with no significant dust deposition below 33 km, based on UK Meteorological Office[10] wind model data and ground-based images of the lingering train[11] taken from Wadi Halfa at sunrise (03:22–03:27 UTC).

Unexpectedly, some meteorites survived the explosion. Fifteen fresh-looking meteorites with a total mass of 563 g were recovered by 45 students and staff of the University of Khartoum during a field campaign on 5–8 December 2008. A second search on 25–30 December (72 participants) raised the total to 47 meteorites and 3.95 kg. Masses range from 1.5 g to 283 g, spread for 29 km along the approach path in a manner expected for debris from 2008 TC_3 (Fig. 1).

Nearly all recovered meteorites show a broken face with no corresponding pieces nearby (Fig. 2). One intact fully crusted meteorite was perfectly oriented in flight, with only a single side exposed to the oncoming air stream and one rotational degree of freedom (Fig. 2e), suggesting that this secondary fragmentation was caused by centrifugal forces or uneven dynamic pressure from rapid tumbling.

Almahata Sitta is a fine-grained fragmental breccia. A small 1.5 g meteorite (no. 7) was broken under 35 lb peak pressure to create a fresh surface for analysis—all results reported here are from this meteorite. It had a tensile strength of only 56 ± 26 MPa, cracking along a white layer, rich in pyroxene, sprinkled with darker areas rich in carbonaceous matter (Fig. 2a).

[1]SETI Institute, Carl Sagan Center, 515 North Whisman Road, Mountain View, California 94043, USA. [2]Physics Department, University of Khartoum, PO Box 321, Khartoum 11115, Sudan. [3]Physics Department, Juba University, Juba, Sudan. [4]NASA Johnson Space Center, Mail Code KT, Houston, Texas 77058, USA. [5]Jacobs Technologies Engineering Science Contact Group (ESCG), Johnson Space Center, Houston, Texas 77058, USA. [6]Department of Chemistry, Fordham University, 441 East Fordham Road, Bronx, New York 10458, USA. [7]Department of Earth and Planetary Sciences, American Museum of Natural History, 79th Street at Central Park West, New York, New York 10024, USA. [8]Geophysical Laboratory, Carnegie Institution of Washington, 5251 Broad Branch Road, NW, Washington DC 20015-1305, USA. [9]Jet Propulsion Laboratory, California Institute of Technology, Pasadena, California 91109, USA. [10]School of Mathematics and Physics, Queen's University Belfast, University Road, Belfast BT7 1NN, UK. [11]Armagh Observatory, College Hill, Armagh BT61 9DG, UK. [12]Department of Physics and Astronomy, University of Western Ontario, London, Ontario N6A 3K7, Canada. [13]ET Space Systems, 5990 Worth Way, Camarillo, California 93012, USA. [14]Sandia National Laboratories, PO Box 5800, Albuquerque, New Mexico 87185, USA. [15]Clay Center Observatory, Dexter and Southfield Schools, 20 Newton Street, Brookline, Massachusetts 02445, USA. [16]Astronomical Institute of the Academy of Sciences, Fričova 298, 25165 Ondřejov Observatory, Czech Republic. [17]Czech Hydrometeorological Institute, Na Sabatce 17, 143 06 Praha 4, Czech Republic. [18]Institut de Mécanique Céleste et de Calcul des Éphémérides, 77 avenue Denfert-Rochereau, 75014 Paris, France. [19]Dutch Meteor Society, Akker 141, 3732 XD De Bilt, The Netherlands. [20]NASA Ames Research Center, Mail Stop 245-6, Moffett Field, California 94035, USA.

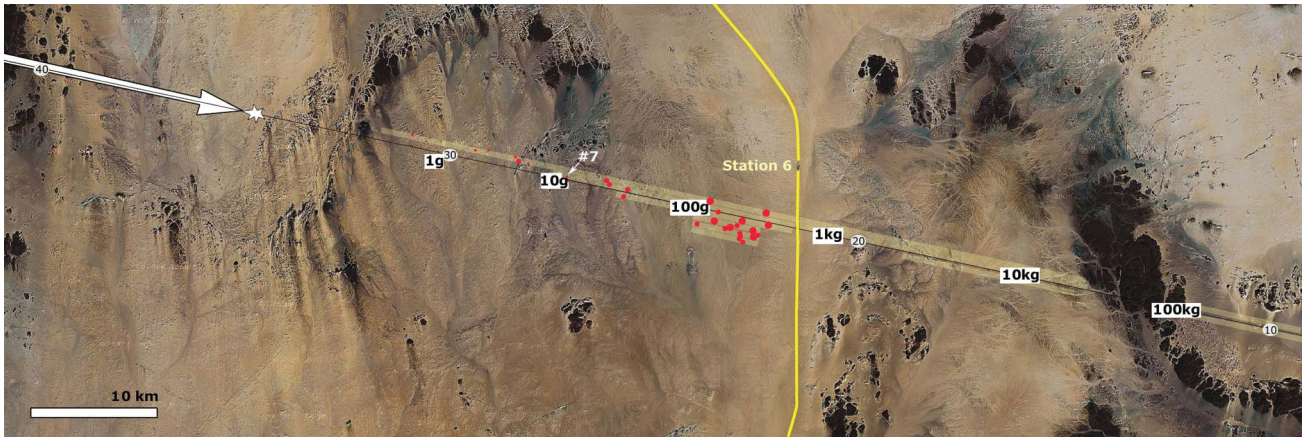

Figure 1 | Map of the Nubian Desert of northern Sudan with the ground-projected approach path of the asteroid and the location of the recovered meteorites. 2008 TC_3 moved from a geodetic longitude of 31.80381° E and latitude of +20.85787° N at 50 km altitude, to 32.58481° E, +20.70569° N at 20 km altitude above the WGS-84 ellipsoid. White arrow represents the path of the 2008 TC_3 fireball with the projected, non-decelerating ground path represented as a thin black line (altitude labels in km, within white ovals). The sizes of the red symbols indicate small (1–10 g), medium (10–100 g) and large (100–1,000 g) meteorites. Our dark-flight calculations show that 270-g fragments would have stopped ablating at around 32 km altitude, falling vertically on the ground at 30–60 m s^{-1}. Labels in white rectangles mark the position where meteorites of indicated masses are predicted to have fallen (calculations assume spheres released at 12.4 km s^{-1} from detonation at 37 km altitude, white star). In light yellow is shown the area that was systematically searched. Special attention was given to possible large fragments further down track, but none were found. Such larger masses would have carried residual forward velocity. The yellow line marks the path of the local train tracks with the location of Station 6 labelled.

Classification of the meteorite was based on oxygen isotopes, bulk chemistry, and mineralogy. The oxygen isotope abundance of two fragments was measured as: $\Delta^{17}O = -0.147‰$ and $-0.501‰$, $\delta^{17}O = 3.90‰$ and $3.56‰$, and $\delta^{18}O = 7.70‰$ and $7.72‰$ relative to Standard Mean Ocean Water (SMOW). A third sample, in contact with fusion crust, gave $\Delta^{17}O = -0.539‰$, $\delta^{17}O = 3.09‰$, and $\delta^{18}O = 6.89‰$ SMOW. These values scatter along the carbonaceous chondrite anhydrous mineral (CCAM) slope of $\delta^{17}O/\delta^{18}O$, on the upper edge of the compositional field of ureilites[12]—see Supplementary Information. Bulk chemistry shows that trace element abundances are achondritic (tabulated in Supplementary Information). Rare earth element (REE) abundances relative to CI chondrites steadily increase with atomic number from 0.1 to 0.6 CI, and possess a distinct negative Eu anomaly, closely resembling the bulk analyses of many ureilites, and generally interpreted as indicative of the material being a residue of partial melting[13,14]. The relatively high (≥0.1 CI) REE abundances in Almahata Sitta are consistent with it being a polymict ureilite, which as a group have higher REE concentrations than the more common monomict ureilites[14]. (The 'polymict' modifier refers to the presence of olivine and pyroxene-rich lithic clasts among ureilitic clasts.) The sample has subrounded mineral fragments and fine-grained olivine aggregates embedded in a cataclastic matrix of ureilitic material (Fig. 3A, B)[15]. Only one case of zoned olivine was found. Shock effects are not apparent. The examined samples have considerable porosity, ranging from 10% to 25%; the walls of pores are commonly coated by anhedral to euhedral crystals of low-calcium pyroxene (Fs_2Wo_3) and olivine ($Fa_{12\text{-}14}$), and in some instances spherules of kamacite and botryoidal masses of Cr-bearing troilite (Fig. 3C). (Here Fs indicates ferrosilite, Wo wollastonite, Fa fayalite, and $Fa_{12\text{-}14}$ indicates 12–14% of this component.) These could be vapour deposits. Aggregates of carbonaceous material, up to 0.5 mm in size, are common and primarily consist of fine-grained graphite, making the rock dark. Some diamond and aliphatic carbon is also present (Fig. 3D).

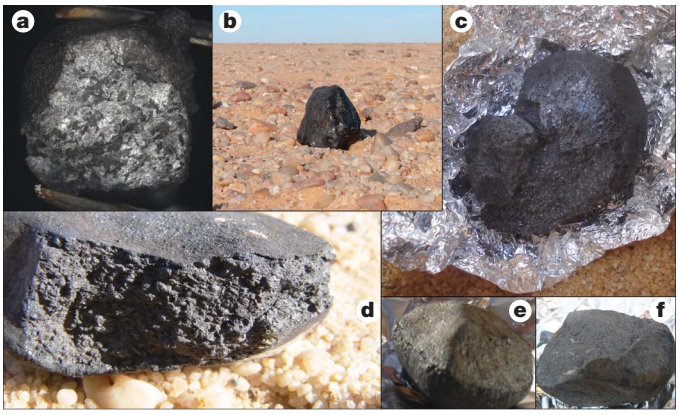

Figure 2 | Macroscopic features of the Almahata Sitta meteorite. **a**, Evidence of clasts in meteorite no. 7 (1 cm diameter) in a fresh fracture surface induced by pressure in the laboratory. **b**, Meteorite no. 15 (4 cm diameter), *in situ*, shows rounded shape of ablated surface. **c**, Meteorite no. 4 (14 g), placed on aluminium foil, shows the dark interior of a surface fractured upon impact. **d**, Meteorite no. 14 (2 × 7 cm), *in situ*, shows millimetre-sized grains in a weathered surface that was broken before impact. **e**, Back side of perfectly oriented meteorite no. 5 (10.9 g), with a front shell exhibiting thick radially flowing crust and a thinly crusted aft-shell. **f**, The very homogeneous course-grained broken surface of large meteorite no. 16 (10 cm diameter).

On the basis of the above information, Almahata Sitta is classified as an anomalous polymict ureilite[14,16]. Ureilites are coarse-grained, ultramafic rocks believed to be either magmatic cumulates or partial melt residues. Mineral compositions of Almahata Sitta are not anomalous, but the textures are, including rare zoning of olivine, larger size carbonaceous aggregates, fine-grained texture, high metal content, and high porosity with possible vapour-phase mineral growth of olivine (consistent with rapid cooling of an impact-produced melt). Other ureilites have a bulk density of 3.05 ± 0.22 g cm^{-3} and an average micro-porosity of 9% (range 6–20%)[17]. The bulk density of Almahata Sitta varies from fragment to fragment. The most precisely measured values (in g cm^{-3}) are 2.10 ± 0.06 (no. 14, 152.6 g) and 2.50 ± 0.08 (no. 16, 171.1 g). Assuming an average ureilite grain density[17] of 3.35 g cm^{-3}, this puts the porosity of Almahata Sitta in the 25–37% range, equal to the high porosities of primitive carbonaceous chondrite meteorites[17].

The recovered meteorites represent only ~0.005% of the initial mass, derived as follows: most are darker than the fractured surface of no. 7 (Fig. 2). Using the V-band albedo of 0.046 ± 0.005, measured for the dark phase of the meteorite, the asteroid's absolute visual magnitude translates to an asteroid diameter of 4.1 ± 0.3 m (ref. 18). If the density were 2.3 ± 0.2 g cm^{-3}, then the pre-atmospheric mass was

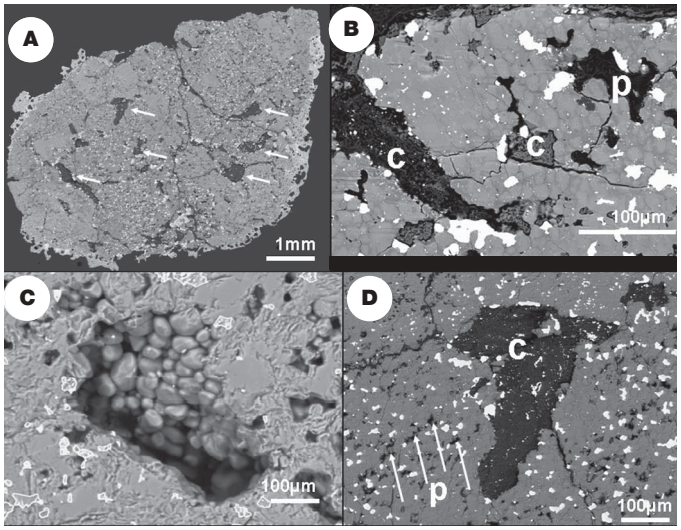

Figure 3 | Petrography[15] of Almahata Sitta. A, Large-scale back-scattered electron view showing high- and low-porosity lithologies; arrows indicate large carbonaceous inclusions; most olivine and pyroxene aggregates have interstitial silicates whose Si-content increases adjacent to metal grains. Mineral fragments include polycrystalline olivine ($Fa_{8\text{-}15}$; CaO = 0.15–0.51 wt%; Cr_2O_3 = 0.03–1.58 wt%), low-calcium pyroxene (Fs_2Wo_5–$Fs_{17}Wo_4$; Cr_2O_3 = 0.33–1.02 wt%), pigeonite ($Fs_{15}Wo_5$–$Fs_{18}Wo_{11}$; Cr_2O_3 = 0.72–1.11 wt%) and carbonaceous aggregates, kamacite ($Fe_{0.92}Ni_{0.08}$–$Fe_{0.96}Ni_{0.04}$) and troilite. Some clasts consist of rounded pyroxene grains containing an abundant Fe-rich nanophase. **B**, Low-porosity grains show rounded crystals. Some carbonaceous areas (c) and a few pores (p) are marked. **C**, Pore containing euhedral to anhedral olivine and pyroxene crystals. **D**, A large carbonaceous aggregate containing dispersed, fine-grained troilite and kamacite, the latter containing Si and P. Note the high porosity (p). Raman spectra measure the carbonaceous grains to be amongst the most graphitic of any meteorite yet studied, with a G band centre and full-width at half-maximum of 1,572 ± 2.1 and 42 ± 5 cm^{-1}, respectively. Imaging Raman shows grain sizes of ~30 μm with slightly higher aromatic order near the rim. Two 10-μm-sized nanodiamonds were imaged in their host material, showing D band peak shifts from latent or biaxial strain. Aliphatic carbon is present too, with weak aliphatic CH-stretch vibration bands peaking at 2,968, 2,921 and 2,852 cm^{-1} (ref. 23).

83 ± 25 t and the kinetic energy of impact $(6.4 \pm 1.9) \times 10^{12}$ J (at 50 km). This compares well with our estimate calculated from acoustic signals from the fireball detected at the Kenyan infrasonic array I32KE: $(6.7 \pm 2.1) \times 10^{12}$ J. Analysis of the bolide light curve shows that the total radiated energy was about 4.0×10^{11} J (ref. 7), which translates empirically[19] to a pre-atmospheric kinetic energy of $\sim 4 \times 10^{12}$ J, in good agreement.

It is unsurprising that such meteorites have not been collected before. The asteroid started to break apart at an altitude of 46–42 km, when the ram pressure was only 0.2–0.3 MPa, and terminated in catastrophic disruption at a pressure of only 1 MPa. The fireball PE-criterion[20], which uses a fireball's observed end height, velocity, mass and entry angle as a proxy for estimating its physical structure, would make this a IIIb/a-type, normally associated with cometary debris (which tends to disrupt at pressures of ≤0.1 MPa). In comparison, the unusual Tagish Lake meteorite was similar in initial mass, entry angle, peak luminosity and light-curve shape, but penetrated deeper into the atmosphere, breaking at 40–29 km, with ablation continuing until 27 km (PE = IIIa/II)[21].

Ureilites were initially thought to derive from S-class asteroids[22] in the Tholen[3] classification of asteroid reflectance spectra. However, the reflectance spectra of 2008 TC_3 and Almahata Sitta meteorite no. 7 are most similar to B or F class asteroids (Fig. 4a). Unlike B-class objects, the meteorite has no hydrated minerals and a modest 3-μm OH-stretch vibration band. This is indicative of minor adsorbed

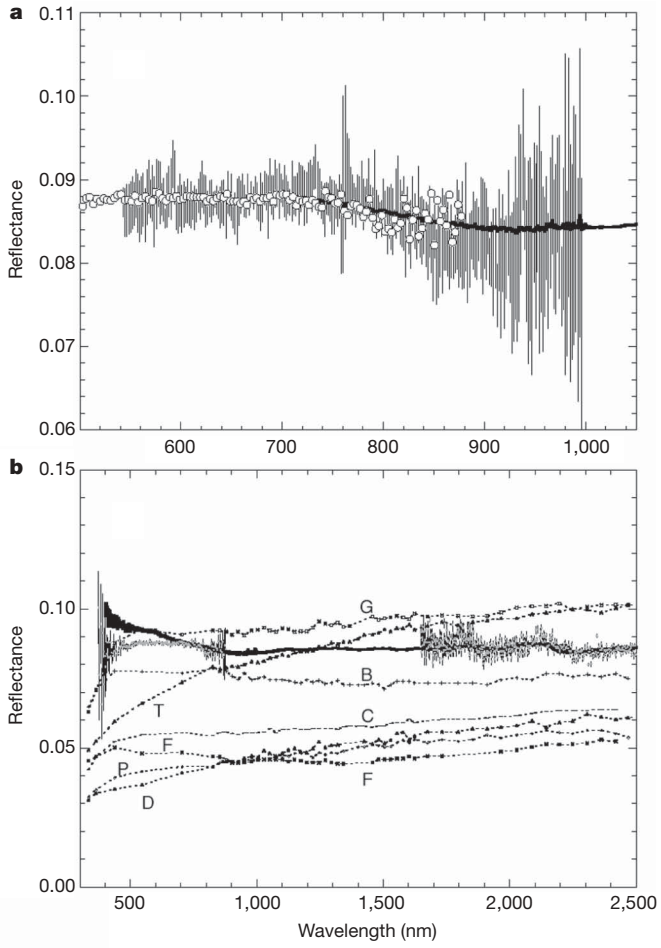

Figure 4 | Meteorite reflectance spectrum compared to that of asteroid 2008 TC_3. a, The meteorite spectrum (circles and thick black line) is measured at 3–7 nm resolution relative to a diffuse reflectance standard. The asteroid spectrum (shown as vertical lines, representing the s.d. of each set of 10 measured points) is measured at 4 nm resolution relative to the solar analogue star 16 Cyg B. We used the 4.2 m William Herschel Telescope and ISIS spectrograph on 6 October at 22:22–22:28 UTC. The Sun–asteroid–Earth phase angle was 18.6°. The asteroid spectrum was scaled vertically to match the albedo of the broken surface of meteorite no. 7 (Fig. 2a). Techniques used to measure the meteorite spectrum: $\lambda < 700$ nm, freshly broken surface no. 7, using a fibre-fed Ocean Optics spectrometer at an illumination angle of 20° and near-perpendicular viewing (circles); $\lambda = 350$–2,500 nm, scraped meteorite surface (thick black line), using a FieldSpec ProFR spectrometer from Analytical Spectral Devices, with reflectance values scaled vertically to match visible albedo data. **b**, Same data (2008 TC_3 shown as grey vertical lines: meteorite no. 7 shown as grey circles and as thick black line over 350–2,500 nm wavelength range) compared to the average reflectance spectra of low albedo asteroid taxonomic classes G, B, C, F, T, P and D[24–27]. Note that individual asteroids within a class show a range of albedo. Long-wavelength near-infrared reflectance was independently measured using a Biorad Excalibur Model 3000 Fourier-transform infrared spectrometer (circles).

telluric water, the meteorite spectra showing none of the substructure diagnostic of many phyllosilicates[23], and implies that 2008 TC_3 was F class. Other low-albedo asteroid types are redder, while B and G classes have a steep drop-off below 400 nm, unlike the meteorite (Fig. 4b)[24–27]. The average asteroid F-class spectrum has a slightly more bluish slope (being more reflective in the blue relative to longer wavelengths) below 700 nm, similar to that of a scraped meteorite surface (Fig. 4b), and a slightly steeper slope above 1,500 nm.

F-class asteroids comprise only ~1.3% of asteroids. Backward integrations of Monte Carlo clones of the orbit of 2008 TC_3 show that there is an evolutionary pathway, driven by interactions with

Earth, originating from orbits similar to only one other known F-class asteroid: the 2.6-km sized (152679) 1998 KU_2. Other candidate parent bodies may be identified in the future.

Received 6 February; accepted 20 February 2009.

1. Lauretta, D. S. & McSween, H. Y. Jr (eds) *Meteorites and the Early Solar System II* (Univ. Arizona Press, 2006).
2. Vernazza, P. *et al.* Compositional differences between meteorites and near-Earth asteroids. *Nature* **454,** 858–860 (2008).
3. Tholen, D. J. in *Asteroids II* (eds Matthews, M. S., Binzel, R. P. & Gehrels, T.) 1139–1150 (Univ. Arizona Press, 1989).
4. Kowalski, R. A. *et al.* in *MPEC 2008–T50* (ed. Williams, G. V.) 1–1 (Minor Planet Center, Smithsonian Astrophysical Observatory, 2008).
5. Yeomans, D. NASA/JPL Near-Earth Object Program Office Statement ⟨http://neo.jpl.nasa.gov/news/news159.html⟩ (6 October 2008).
6. Chesley, S., Chodas, P. & Yeomans, S. NASA/JPL Near-Earth Object Program Office Statement ⟨http://neo.jpl.nasa.gov/news/2008tc3.html⟩ (4 November 2008).
7. Pravec, P. *et al.* Tumbling asteroids. *Icarus* **173,** 108–131 (2005).
8. Brown, P. G. *US Government release: Bolide detection notification 2008–282* (15 October 2008); ⟨http://aquarid.physics.uwo.ca/~pbrown/usaf/usg282.txt⟩.
9. Borovicka, J. & Charvat, Z. 2008 TC_3. *IAU Circ. No.* 8994 (2008).
10. Swinbank, R. & O'Neill, A. A. A stratosphere-troposphere data assimilation system. *Mon. Weath. Rev.* **122,** 686–702 (1994).
11. Elhassan, M., Shaddad, M. H. & Jenniskens, P. On the trail of 2008 TC3. (Astronomy Picture of the Day, NASA Goddard Space Flight Center, 8 November 2008); ⟨http://apod.nasa.gov/apod/ap081108.html⟩.
12. Clayton, R. N. & Mayeda, T. K. Oxygen isotope studies of achondrites. *Geochim. Cosmochim. Acta* **60,** 2681–2708 (1996).
13. Goodrich, C. A., Van Orman, J. A. & Wilson, L. Fractional melting and smelting on the ureilite parent body. *Geochim. Cosmochim. Acta* **71,** 2876–2895 (2007).
14. Mittlefehldt, D. W., McCoy, T. J., Goodrich, C. A. & Kracher, A. Non-chondritic meteorites from asteroidal bodies. *Rev. Mineral.* **36,** 1–195 (1998).
15. Zolensky, M. *et al.* Andreyivanovite: A second new phosphide from the Kaidun meteorite. *Am. Mineral.* **93,** 1295–1299 (2008).
16. Goodrich, C. A. Ureilites: A critical review. *Meteoritics* **27,** 327–353 (1992).
17. Britt, D. T. & Consolmagno, S. J. Stony meteorite porosities and densities: A review of the data through 2001. *Meteorit. Planet. Sci.* **38,** 1161–1180 (2003).
18. Pravec, P. & Harris, A. W. Binary asteroid population. I. Angular momentum content. *Icarus* **190,** 250–259 (2007).
19. Brown, P., Spalding, R. E., ReVelle, D. O., Tagliaferri, E. & Worden, S. P. The flux of small near-Earth objects colliding with the Earth. *Nature* **420,** 294–296 (2002).
20. Ceplecha, Z. *et al.* Meteor phenomena and bodies. *Space Sci. Rev.* **84,** 327–471 (1998).
21. Brown, P. G., ReVelle, D. O., Tagliaferri, E. & Hildebrand, A. R. An entry model for the Tagish Lake fireball using seismic, satellite and infrasound records. *Meteorit. Planet. Sci.* **37,** 661–675 (2002).
22. Gaffey, M. J. *et al.* Mineralogic variations within the S-type asteroid class. *Icarus* **106,** 573–602 (1993).
23. Sandford, S. A. The mid-infrared transmission spectra of Antarctic ureilites. *Meteoritics* **28,** 579–585 (1993).
24. Hiroi, T., Zolensky, M. E. & Pieters, C. M. Discovery of the first D-asteroid spectral counterpart: Tagish Lake meteorite. *Lunar Planet. Sci. Conf.* **32,** abstr. 1776 (2001).
25. Tholen, D. J. *Asteroid Taxonomy from Cluster Analysis of Photometry.* Ph.D. Thesis, Univ. Arizona (1984).
26. Zellner, B., Tholen, D. J. & Tedesco, E. F. The eight-color asteroid survey: Results for 589 minor planets. *Icarus* **61,** 335–416 (1985).
27. Bell, J. F. Mineralogical clues to the origins of asteroid dynamical families. *Icarus* **78,** 426–440 (1989).

Supplementary Information is linked to the online version of the paper at www.nature.com/nature.

Acknowledgements We thank the University of Khartoum for support of the field campaigns, and students and staff of the Physics Department of the Faculty of Sciences for their efforts to recover the meteorites. P.J. is supported by the NASA Planetary Astronomy program. D.R. acknowledges the support of NASA's Cosmochemistry program (grant NNX07AI48G). A. Alunni, J. Travis-Garcia and L. Hofland of NASA Ames Research Center, and J. Herrin of NASA Johnson Space Flight Center, provided laboratory assistance. The work conducted at JPL/Caltech was under contract with NASA. The William Hershel Telescope is operated on the island of La Palma by the Isaac Newton Group in the Spanish Observatorio del Roque de los Muchachos of the Instituto de Astrofísica de Canarias.

Author Contributions P.J., M.H.S., D.N., S.E. and A.M.K. led the field search for meteorites. M.E.Z., L.L. and G.A.R. performed the petrographic analysis. J.M.F. performed the trace element bulk chemistry analysis. D.R. performed the oxygen isotope analysis. A.S. performed the Raman analysis. S.R.C. calculated the orbit and ground track. A.F., S.D., H.H.H. and G.R. observed and analysed the astronomical spectrum. P.G.B. analysed the infrasound data. P.G.B., W.N.E. and P.J. performed dark-flight calculations. S.P.W., E.T., M.B.B. and R.E.S. facilitated and analysed the US Government satellite observations. R.D. and M.K. observed the asteroid light curve, which was analysed by P.P., J.B. and Z.C. analysed the Meteosat 8 observations. P.J. and J.V. investigated the link with possible other parent bodies. J.K. provided wind model data. J.A. and P.J. analysed train wind drift. J.L.B. and P.J. measured reflection spectra of the meteorite. R.L.M. and P.J. obtained optical imaging of the meteorite. S.A.S., S.N.M., M.N. and P.J. performed the mid-infrared analysis.

Author Information Reprints and permissions information is available at www.nature.com/reprints. Correspondence and requests for materials should be addressed to P.J. (Petrus.M.Jenniskens@nasa.gov).